

## Evolution of the magnetization depth profile of Fe/Cu(100) films upon thermal annealing

J. Shen, Ch. V. Mohan, P. Ohresser, M. Klaua, and J. Kirschner  
*Max-Planck-Institut für Mikrostrukturphysik, Weinberg 2, 06120 Halle/Saale, Germany*  
(Received 11 September 1997; revised manuscript received 5 November 1997)

The annealing effect on the magnetic and structural properties of Fe/Cu(100) ultrathin films has been studied. For films below 5 ML, their magnetization and Curie temperature are reduced considerably after annealing. We explain the reduction as a result of the transition from a high-moment ferromagnetic phase to a nonferromagnetic phase in the inner layers of the Fe films after annealing. Supporting evidence comes from the low-energy electron-diffraction study, which indicates a structural relaxation from a tetragonally distorted fct structure to a true fcc structure in the inner layers of the Fe films. The surface layers of the Fe films, after annealing, are still expanded, providing the main contribution to the remaining magnetization and nonzero Curie temperature of the annealed Fe films. [S0163-1829(98)00821-2]

### I. INTRODUCTION

The ultrathin film system of epitaxially grown face-centered-cubic (fcc) Fe on Cu(100) has been extensively studied in recent years.<sup>1-8</sup> It has been observed that this system is metastable upon variation of thickness. The structure of the room-temperature as-grown films is face-centered tetragonal (fct) with buckling below 5 ML.<sup>9</sup> Between 5 and 11 ML,<sup>3</sup> the films have a fct structure in the top layers but a fcc structure in the layers underneath. The structure of the films finally transforms to a much more stable body-centered-cubic (bcc) modification above 11 ML.<sup>10</sup> The fcc to bcc structural transformation is largely driven by the energy difference between fcc and bcc Fe. The transformation starts with forming dislocations at about 4 to 5 ML and proceeds by following the martensitic path.<sup>2,11</sup> The appearance of the dislocations is likely associated with the fct→fcc structural relaxation which occurs between 4 and 5 ML.

The structural changes of the Fe/Cu(100) system have strong influence on its magnetic behavior. In the fct thickness regime (<5 ML), the films have a uniform high-spin ferromagnetic phase.<sup>6</sup> The easy magnetization axis is perpendicular to the film surface.<sup>1</sup> Between 5 and 11 ML, while the easy magnetization axis is still perpendicular, the magnetization of the films become nonuniform in depth.<sup>1,4</sup> It has been observed that in this thickness regime only the topmost layer has a high-spin ferromagnetic phase while the layers underneath become nonmagnetic or antiferromagnetic depending on the temperature.<sup>1,4,7,8</sup> As a result, the total magnetization of the films (from 5 to 11 ML) has only a value about 30–40% of that of the 4 ML film. The reduction of the magnetization has been generally believed to result from the fct to fcc structural relaxation,<sup>3</sup> which agrees with a theoretical prediction of the magnetic moment–atomic volume relationship of fcc Fe.<sup>12</sup>

The metastability of the Fe/Cu(100) films has also shown up when varying the temperature. Zharnikov *et al.*<sup>13</sup> have shown that a 4 ML film undergoes a reversible fct to fcc structural relaxation during temperature cycle from 160 to 370 K. Further increasing the annealing temperature above 400 K results in significant Fe-Cu interdiffusion.<sup>14</sup> It has

been realized for some years that after annealing the surface layers of the films become copper rich.<sup>15</sup> Our recent scanning tunneling microscopy (STM) study<sup>16</sup> has unambiguously shown that the mechanism of the copper diffusion is a surface diffusion via rectangular pits which are formed during annealing. In Refs. 16 and 17 these pits were termed as “pinholes” which did not reflect the fact that the lateral extension of the pits is usually 5–10 times larger than their vertical extension. Therefore in this paper we will rename them “pits” instead of “pinholes.” The diffused copper from the pits covers the surface of the films and forms a Cu/Fe/Cu sandwich structure. This also implies that the equilibrium of the Fe/Cu(100) films is neither two-dimensional layers nor three-dimensional clusters of Fe on the substrate, but rather a Cu/Fe/Cu sandwich structure.

It is important to know the atomic structure and in particular the magnetic properties of the annealed Fe/Cu(100) films. This is not only because of the interest of understanding the properties of the Fe/Cu(100) films at equilibrium, but also because of the fact that thermal annealing is a general process during the magnetic measurements such as Curie temperature. Apparently the physical meaning of the measured magnetic quantities at high temperatures will only be well understood by studying the annealing effect. Furthermore, a study of the annealing effect on the structure and magnetism of the Fe/Cu(100) films will also serve as guidance for some other magnetic systems such as Co/Cu(100) (Ref. 17) and Fe/Au(100),<sup>18</sup> where a similar diffusion mechanism holds.

Therefore, following our previous work on morphology,<sup>16</sup> in this paper we describe the influence of annealing on the magnetization depth profile of the Fe/Cu(100) films after annealing, a subject which has hardly been touched in this “ever green” system. We have observed that the Curie temperature and the total magnetization of the Fe films become remarkably small after annealing. We interpret these changes as a result of the transition from a high-spin ferromagnetic state to a low-spin ferromagnetic or even a nonferromagnetic state in the inner layers of the Fe films, which is strongly supported by structural data from our low-energy electron-diffraction (LEED) studies.

## II. EXPERIMENTAL DETAILS

The experiments were performed in an ultrahigh vacuum (UHV) multichamber system including a molecular-beam-epitaxy preparation chamber, a STM chamber, an analysis chamber equipped with facilities for Auger electron spectroscopy (AES), LEED and thin-film growth, and a magneto-optical Kerr effect (MOKE) chamber. The base pressure of the individual chambers is better than  $5 \times 10^{-11}$  mbar. A fully automatic video-LEED system<sup>19</sup> has been used for recording LEED images as well as for measuring intensity vs energy ( $I/V$  LEED) curves. The sample was prepared in the analysis chamber. Prior to film deposition the copper substrate was cleaned by  $\text{Ar}^+$  sputtering followed by annealing at 870 K. After several cycles of this procedure we have achieved a clean and flat substrate. Contamination-free Auger spectrum, sharp LEED spots and large atomically flat terraces (on the order of several hundred nanometers) under STM all prove the high quality of the copper substrate. The Fe films were prepared from an iron wire (5N) heated by  $e$ -beam bombardment. During deposition the substrate was kept at room temperature ( $300 \pm 5$  K), and the vacuum pressure rose from  $7 \times 10^{-11}$  to  $2 \times 10^{-10}$  mbar at a typical evaporation rate of 0.2 monolayer/min. The well-cleaned Fe source and the excellent vacuum have guaranteed the cleanliness of the Fe films as examined by the AES ( $<0.5$  at. % of carbon contamination).

After the film preparation, the LEED and  $IV$ -LEED measurements were taken immediately from the as-grown films. Then the sample was transferred to the MOKE chamber. Magnetic data were recorded *in situ* from films both before and after annealing. The annealing temperature was typically about 490 K though other temperatures have also been tried. The heating rate was about 10 K/min in the temperature range between 300 and 490 K, allowing the maximum pressure to be maintained below  $3 \times 10^{-10}$  mbar. The copper diffusion process has been observed to be dependent on both the annealing temperature and the heating rate, and a detailed discussion will be presented in a forthcoming paper.<sup>20</sup> The LEED and  $IV$ -LEED analysis of the annealed samples were finally done in the analysis chamber. STM and AES have also been used to examine the number of pits and the amount of diffused copper in the annealed films, and similar results to those described in Ref. 16 were obtained.

## III. REDUCED MAGNETIZATION AND ITS STRUCTURAL ORIGIN

Let us first discuss the changes of the magnetic properties after annealing. For convenience, we will concentrate on films with thickness of 3 and 4 ML, while we note here that the characteristic features are general for all films between 2 and 5 ML. Figure 1 shows the measured Kerr hysteresis curves of the 3 and 4 ML films before and after annealing. All the curves were recorded in the polar geometry at about 150 K. The hysteresis loops of the films before annealing have a well-defined rectangular shape, while after annealing the corners of the hysteresis become somewhat rounded. In both cases the remanent magnetization ( $M_r$ ) equals 100% of the saturation magnetization ( $M_s$ ), indicating that the easy magnetization axis remains to be perpendicular to the surface

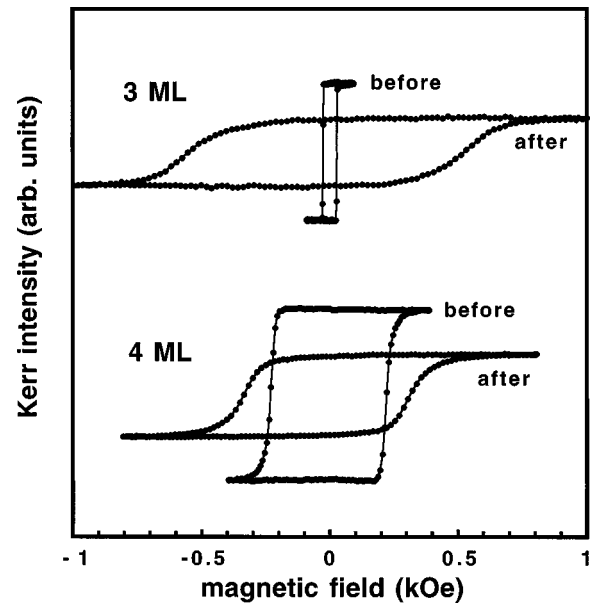


FIG. 1. Polar MOKE hysteresis loops of 3 and 4 ML Fe/Cu(100) film before and after annealing. The loops were recorded at 150 K. Annealing has caused an increase of the coercive field  $H_c$  but a decrease of the saturation magnetization  $M_s$  and remanence  $M_r$ .

after annealing. This has also been confirmed by the in-plane MOKE measurements (not shown here), which show a typical hard-axis behavior of the film.

Before annealing, the 3 ML film has a much smaller coercivity ( $H_c$ ) than that of the 4 ML film. Generally a smaller  $H_c$  is an indication of a more perfect structure which has less defects to pin the domain motion. However, according to our previous STM results, the surface roughness of the 3 and 4 ML films are small and comparable.<sup>16</sup> The large difference between the  $H_c$  values of the 3 and 4 ML films must come from other factors causing structural imperfection. Previous LEED (Ref. 3) and STM (Ref. 2) studies indicate that above 4 ML the Fe films undergo a fct $\rightarrow$ fcc structural relaxation and a fcc $\rightarrow$ bcc phase transformation simultaneously. Both processes cause structural imperfection: the former results in different interlayer spacing for different layers while the latter generates dislocations. It is these imperfections that are likely responsible for the enhanced coercivity of the 4 ML film.

After annealing the hysteresis loops are widened with a distinctly larger  $H_c$  than that of the films before annealing. The effect is particularly strong for the 3 ML film. At 150 K, the coercive field drastically increases by a factor of more than 20, from 25 Oe before annealing to 535 Oe after annealing. For the 4 ML film, the increase of  $H_c$  is much less pronounced, from 230 Oe before annealing to 340 Oe after annealing. It is interesting to note that after annealing, the 4 ML film has a smaller  $H_c$  than the 3 ML film though the situation is just reverse before annealing.

Another visible effect of annealing, from Fig. 1, is the decrease of the magnetization of the films. At 150 K, the measured magnetization appears to have decreased by a factor of 2 for both 3 and 4 ML films. A more strict comparison of the magnetization requires also the knowledge of the Curie temperature ( $T_c$ ), because the chosen temperature (150

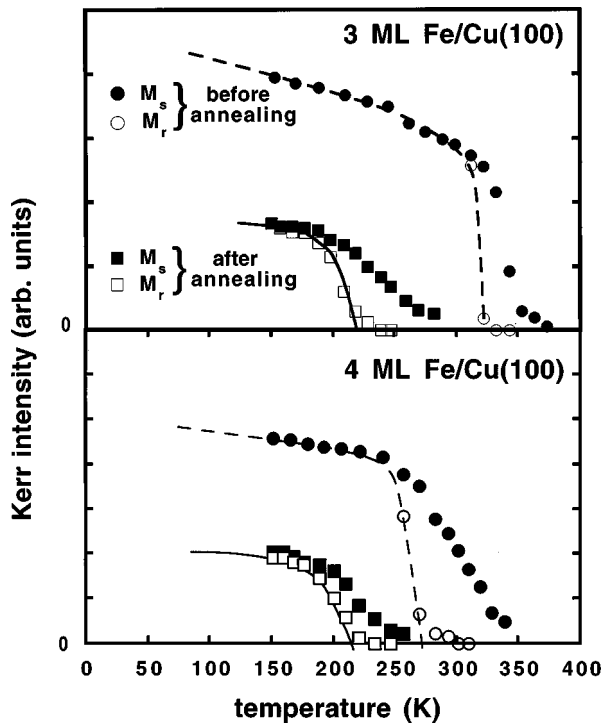


FIG. 2. Temperature dependence of the saturation  $M_s$  and remanent magnetization  $M_r$  of the 3 ML (upper panel) and 4 ML (lower panel) Fe/Cu(100) film before and after annealing. The dashed and the full lines correspond to  $M_r$  before and after annealing, respectively, and are only for guiding the eyes.

K) for comparison must be well below  $T_c$  to avoid any uncertainties caused by the rapid fall of the magnetization in the vicinity of  $T_c$ . To determine  $T_c$ , we have measured the temperature dependence of  $M_s$  and  $M_r$ . The values of the  $M_s$  and  $M_r$  were taken from the hysteresis loops. The results for the 3 ML (upper panel) and 4 ML film (lower panel) are shown in Fig. 2. It remains a matter of dispute whether one should use  $M_s$  or  $M_r$  to determine the precise value of  $T_c$ . In principle, these two should yield the same result as far as a film with a perfect structure is concerned. The difference between the temperature dependence of  $M_s$  and  $M_r$  often reflects the deviation of the structure of the film from the perfect order. It has been suggested by Kohlhepp *et al.*,<sup>21</sup> that the  $M_s$  vs  $T$  curve would yield a more reliable  $T_c$  if the saturation field remains reasonably small. However, all the  $M_s$  curves except that of the 3 ML film before annealing in Fig. 2 were measured under large field, which requires the Curie temperature to be determined by the  $M_r$  vs  $T$  curve. The 3 ML film before annealing has a rather small saturation field (less than 100 Oe), but its structural perfection results in only a small difference between the  $M_s$  and  $M_r$  curves. Therefore, for consistency we will use the  $M_r$  vs  $T$  curves to determine  $T_c$  in all four cases. The obtained  $T_c$  values for the 3 and 4 ML films are 325 and 275 K before annealing, and 220 and 215 K after annealing, respectively. Apparently the Curie temperature of the Fe films has been considerably reduced after annealing. It is also interesting to note here that the 3 and 4 ML annealed films have a close  $T_c$  value around 220 K.

With the knowledge of the temperature dependence of  $M_s$ , we can extrapolate  $M_s$  at 0 K, i.e., the spontaneous

magnetization, from Fig. 2. We estimate that the magnetization (0 K) of the 3 ML film after annealing is about 40% of that of the film before annealing. By the same way we determined that the magnetization of the 4 ML annealed film reduces to about 45% of the original value.

Two possible mechanisms could be responsible for the decrease of the magnetization after annealing. The first one is the copper diffusion towards the top of the film surface.<sup>16</sup> It has been observed recently that capping layers on top of a 3 ML Fe film results in a reduction of the magnetization and the Curie temperature depending on the copper thickness.<sup>22</sup> Moreover, in Ref. 16 we have demonstrated that the diffused copper mixes with the top Fe layers and form Fe-Cu surface alloy. Theoretically for an atomically ordered Fe-Cu alloy,<sup>23</sup> the magnetic moment of Fe atoms is only slightly smaller than in pure Fe once the copper concentration is under 50%. As no such ordered alloy exists in the bulk, one could only produce Fe-Cu alloys either by stabilizing fcc Fe clusters in a Cu matrix, i.e., a cluster-type alloy, or by epitaxially stacking monoatomic Fe and Cu layers.<sup>24</sup> The former is antiferromagnetic with a Néel temperature of about 67 K,<sup>25</sup> while the latter appears to be ferromagnetic (its magnetic moment needs to be further examined<sup>24</sup>). The Fe-Cu surface alloy in the annealed Fe/Cu(100) films consists of Fe-rich and Cu-rich patches,<sup>16</sup> which is in between the ordered alloy and the cluster alloy. The reduced magnetization of the annealed Fe films can also be partly caused by the alloy formation if one assumes the Fe magnetic moment to be small in the alloy.

The second possible mechanism would be a magnetic phase transition. By annealing the Fe films may transform from the high-spin ferromagnetic phase to a low-spin ferromagnetic phase or a nonmagnetic phase. Because the close connection between the magnetic moment and atomic volume of fcc Fe, the magnetic phase transition should result in or originate from a change of lattice constant. If the films transform to a low-spin phase, the lattice constant of the whole films should become uniformly smaller. If the films transform to a nonmagnetic phase, parts of the films must be still ferromagnetic, otherwise there would be no magnetic signal detectable after annealing. Therefore only the nonmagnetic part of the films would have a reduced interlayer distance while the ferromagnetic part remains unchanged.

To decide which of the above two mechanisms is responsible for the reduction of the magnetization, it is important to know (1) the exact amount of diffused copper onto the surface; (2) the extent of the change of the lattice constant. A general method to determine the copper diffusion is AES. But in the Fe/Cu(100) system a quantitative analysis by AES turns out to be difficult because of the formation of the Fe-Cu alloy. We therefore decided to use STM to determine the amount of diffused copper. As an example, Fig. 3 shows STM topography images of a 3 ML Fe/Cu(100) film before (a) and after (b) annealing. Before annealing, the film shows a good layer-by-layer morphology as the third layer has been more than 95% filled. After annealing, pits (dark patches) have been formed in the film. Between the pits there exist many small sub-monolayer-deep depressions, which are considered as characteristic features of the Fe-Cu surface alloy.<sup>16</sup> The total material diffused out of the pits can be determined by calculating the volume of the pits. In order to reduce the statistical error, we made our calculation on more

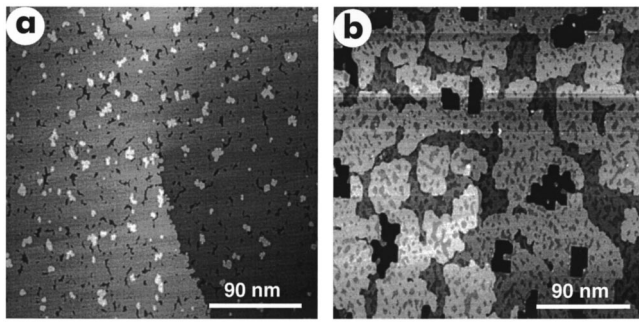


FIG. 3. STM topography images of a 3 ML Fe/Cu(100) film before (a) and after (b) annealing. Before annealing the film exhibits three exposed layers, i.e., second (dark), third (grey), and fourth (bright) layer. The third layer contributes more than 95% of the total area. After annealing, several nanometer-deep pits (dark patches) have been formed as a result of the copper diffusion towards the top of the surface. Submonolayer-deep depressions are clearly visible between the pits. These depressions are characteristic features of the Fe-Cu surface alloy, see also, Ref. 16.

than 20 images ( $300 \times 300 \text{ nm}^2$ ) taken from various surface locations. Subtracting the Fe part (0.1 and 0.07 ML for 3 and 4 ML film, respectively), we estimated the amount of diffused copper to be about 0.6 and 0.4 ML for the 3 and 4 ML Fe film, respectively. Above 4 ML the copper diffusion becomes insignificant as the films are thick enough to preclude pit formation.

The structural changes of the films upon annealing have been analyzed by LEED and *IV*-LEED. Figure 4 shows the LEED patterns (normal incidence) recorded before (left column) and after annealing (right column) of the 3, 4, and 5 ML Fe/Cu(100) films. Before annealing, the 3 and 4 ML films exhibit a complicated  $(5 \times 1)$  superstructure, while the 5 ML film shows a  $(2 \times 1)_{p2mg}$  type of superstructure. These results are consistent with previous LEED studies of the room-temperature as-grown Fe/Cu(100) films.<sup>26,27</sup> The  $(5 \times 1)$  superstructures have been considered as a reflection of the buckling of the surface atoms.<sup>27</sup> In this respect at room-temperature the growth of Fe on Cu(100) is by no means a real pseudomorphic growth.

Stark change of the LEED patterns has been observed for the films after annealing, as shown in the right column of Fig. 4. None of the original superstructures is visible in the annealed films. Instead, another type of superstructure,  $c(2 \times 2)$ , appears in the LEED patterns. The relative intensity of the  $c(2 \times 2)$  superstructure spots over the substrate spots decreases with increasing Fe thickness, reaching nearly the level of the background at 5 ML. In this system, the  $c(2 \times 2)$  superstructure could be caused by two optional mechanisms. First, it is known<sup>28</sup> that the adsorption of the residual gas in vacuum ( $\text{O}_2$ , CO, etc.) could cause such a superstructure on the surface of the Fe/Cu(100) films. During annealing the vacuum pressure often increases slightly, which will unavoidably result in a bit larger amount of adsorption than normal. Our AES data confirm the weight of carbon and oxygen peaks to slightly increase after annealing (but by a factor of less than 2 corresponding to less than 1% carbon contamination). Second, the  $c(2 \times 2)$  superstructure may simply reflect the order of the Fe-Cu surface alloy which is formed due to the copper diffusion during annealing. The

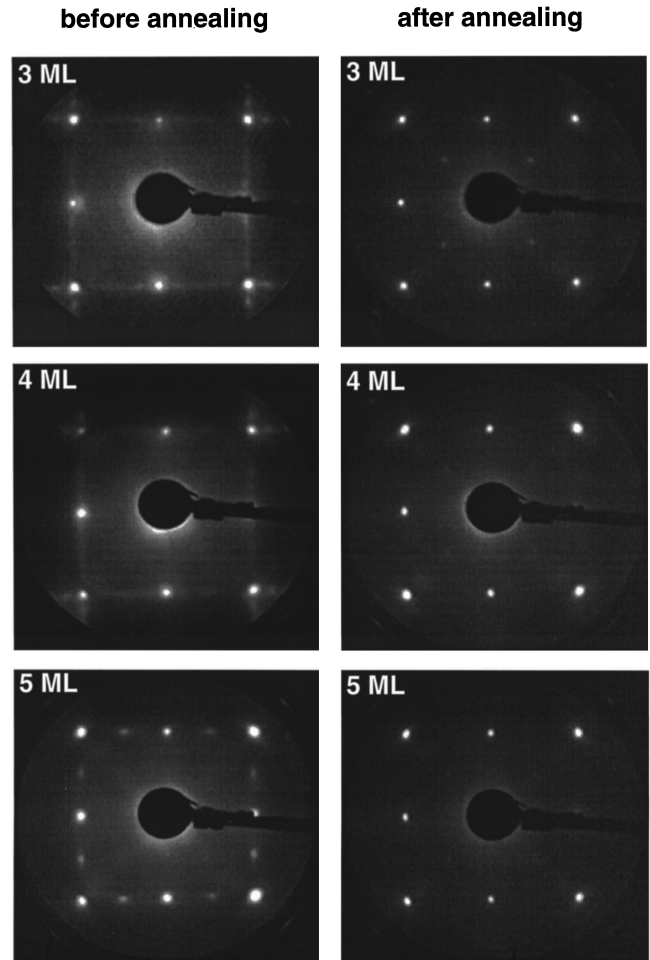


FIG. 4. LEED patterns of Fe/Cu(100) films before annealing (left column) and after annealing (right column). All pictures were recorded at 108 eV. Before annealing, the 3 and 4 ML films exhibit  $(4 \times 1)$  and  $(5 \times 1)$  superstructures, while the 5 ML film shows a  $(2 \times 1)_{p2mg}$  structure. After annealing, all the films have a  $c(2 \times 2)$  superstructure whose intensity relative to that of the substrate spots decreases with increasing thickness.

latter could explain the fact that the intensity of the superstructure spots decreases with increasing thickness, since the amount of diffused copper, thus the Fe-Cu surface alloy, decreases with increasing thickness. The adsorption of the residual gases on the films' surface, however, should not depend on the thickness. Therefore we tentatively attribute the origin of the  $c(2 \times 2)$  superstructure to the Fe-Cu surface alloy. At this point we do not know the exact atomic arrangement which causes the  $c(2 \times 2)$  pattern.

In any case, we can conclude that there is no buckling of the surface atoms of the annealed films because of the disappearance of the  $(5 \times 1)$  superstructure. This, to some extent, is an indication that annealing improves the lateral order of the Fe films with respect to that of the copper substrate, except that the surface layer is affected by the Fe-Cu surface alloy. Such an improvement, according to our *IV*-LEED results, is not only limited in the lateral direction, but also in the vertical direction of the Fe films.

Figure 5 shows the LEED (00) beam intensity as a function of the beam energy. The  $I(E)$  spectra of the Fe/Cu(100) films before and after annealing are displayed in the lower

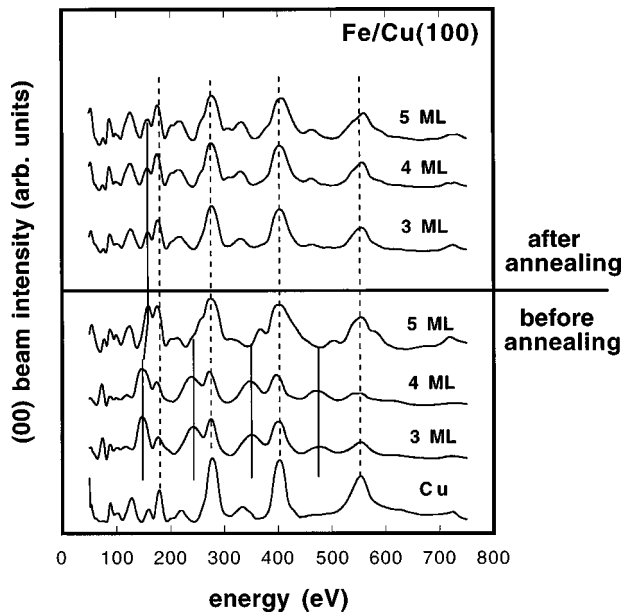


FIG. 5.  $I(E)$  spectra of the (00) beam for Fe/Cu(100) films before (lower panel) and after (upper panel) annealing. The dashed lines indicate the fcc peak positions as obtained from that of the copper substrate, while the full lines mark the fct peaks of the Fe films. Before annealing, the 3 and 4 ML films have four fct peaks each, and the 5 ML film has only two low-energy fct peaks. After annealing, all the films have only two low-energy fct peaks, whose intensity is even smaller than those of the 5 ML film before annealing.

and the upper panels, respectively. In this case the primary beam is about  $6^\circ$  off the surface normal lying in the (001) plane. Before annealing, the spectra of the 3 and 4 ML films are characterized by two families of peaks which are marked by solid and dashed lines, respectively. The peaks on the dashed lines have nearly the same energy positions as those of the copper substrate. These peaks will be referred to as fcc peaks, since they stand for an interlayer distance which is close to that of the fcc substrate. The peaks on the solid lines clearly have lower energy positions than the fcc peaks. Under the assumptions of the kinematic theory, these peaks correspond to an interlayer distance which is larger than that of the substrate. These peaks will be referred to as fct peaks. Within the kinematic model we have calculated the interlayer distance, which is  $1.82 \text{ \AA}$  for the fcc and  $1.95 \text{ \AA}$  for the fct peaks. For the films below 5 ML, the intensity of the fcc peaks decreases with increasing thickness, hinting that these peaks are likely contributed from the substrate. The fct peaks, on the other hand, reflect the real interlayer distance of the Fe films below 5 ML. The existence of the fct peaks and the superstructure suggests that the Fe films ( $<5 \text{ ML}$ ) have adopted neither the lateral nor the vertical lattice constant of the copper substrate.

Increasing thickness up to 5 ML affects the fct peaks strongly. The three high-energy fct peaks disappear, and the intensity of the two low-energy fct peaks become weaker and shift slightly towards higher energies. Since the high-energy peaks are contributed by electrons with longer escape length, the disappearance of these peaks indicates that the bulk layers of the Fe films are no longer vertically expanded. The surface layers, however, are still expanded as evidenced by

the existence of the low-energy fct peaks.

After annealing, the  $I(E)$  spectra of the 3, 4, and 5 ML films (upper panel in Fig. 5) are remarkably similar to the spectrum of the 5 ML film before annealing. This indicates that the inner layers of the annealed Fe films have the same interlayer distance as copper. In other words, annealing results in a structural relaxation, from fct to fcc, in the inner layers of the 3 and 4 ML Fe films. The inner layers of the 5 ML film already have the fcc structure before annealing, thus no further structural change occurs upon annealing. The surface layers of the annealed Fe films appear to be still expanded, though the intensity of the two low-energy fct peaks is even smaller than for the 5 ML film before annealing.

The following picture can be drawn from our STM and LEED data regarding the annealing effect on the structure of the room-temperature grown Fe/Cu(100) films. For the films below 5 ML, upon annealing, rectangular pits are formed in the Fe films, serving as channels for the diffusion of the substrate copper onto the top of the surface. The diffused copper mixes with the surface layers of the Fe films and forms an Fe-Cu surface alloy. A fct  $\rightarrow$  fcc structural relaxation occurs in the bulk layers of the Fe films, while the structure of the surface layers remains fct-like. At or above 5 ML, the films become thick enough to preclude the pit formation on the atomically flat terraces though a few pits may exist at some weak points of the films. A detailed discussion of the origin of these annealing effects will be given in Sec. IV.

#### IV. DISCUSSION

As mentioned, the amount of diffused copper for the 3 ML film is about 0.6 ML. Deliberately capping such an amount of copper onto the as-grown 3 ML Fe film would lead to a magnetization reduction by only about 15%,<sup>22</sup> which is not sufficient to explain the observed reduction by a factor of 2. The fct to fcc structural relaxation in the inner layers of the annealed Fe films, however, could well explain the reduction of the total magnetization after annealing. The contracted inner layers, with a smaller atomic volume, are likely converted into a nonferromagnetic state, i.e., paramagnetic or antiferromagnetic state, whose magnetization is significantly smaller than the high-spin ferromagnetic state. As for the topmost layers, we cannot unequivocally determine their magnetization. On one hand, they remain expanded after annealing, which should still result in the high-spin ferromagnetic state. On the other hand, they are present in a form of a Fe-Cu surface alloy instead of pure Fe. The magnetic moment of the Fe atoms in the Fe-Cu alloy might decrease depending on the Cu concentration as well as on the structure of the alloy. As mentioned earlier, so far there has been no experimental or theoretical work discussing the magnetic moment of Fe atoms in the type of Fe-Cu alloy observed in the annealed Fe/Cu(100) films, i.e., a surface alloy formed by Fe-rich and Cu-rich patches. To match the measured magnetization of the annealed Fe films, we suggest the following model of the magnetization depth profile of the annealed Fe films.

We first discuss the 3 ML film. The annealed 3 ML Fe film become virtually 3.7 ML thick owing to the additional

material diffused out of the pits. This material includes 0.6 ML of Cu and 0.1 ML of Fe. If the diffused 0.6 ML Cu mixes only with the topmost layer of Fe, the alloy would contain 35% of Cu and 65% of Fe. The calculation in Ref. 22 indicates that the magnetic moment of Fe atoms will only reduce very little once the Fe concentration exceeds 50%. Therefore, in this case the 1.7 ML topmost Fe-Cu alloyed layers should have a magnetization similar to that of 1.1 ML Fe in the high-spin phase. The magnetization of the annealed film is about 37% of that of the 3 ML high-spin Fe before annealing, which agrees well with the 40% value obtained from Fig. 2. The bottom two layers in the annealed film should possess small or even zero net magnetization. The detailed magnetic structure, whether it is low-spin ferromagnetic or paramagnetic, remains unclear.

The same model can be applied to the 4 ML film. After annealing, 0.4 ML of diffused Cu forms an alloy with the topmost Fe layer. Here the magnetization of the 1.4 ML Fe-Cu alloy would equal roughly that of 1 ML high-spin ferromagnetic Fe, which is 25% of the magnetization of the 4 ML film before annealing. Since Fig. 2 (bottom panel) shows that the magnetization of the 4 ML film after annealing is about 45% of that before annealing, one has to assume that the three Fe layers below the alloyed layers of the annealed film have a nonzero net magnetization. Such a nonzero net magnetization can be resulted from two types of spin alignment in the three inner layers: (1) a perfect layered antiferromagnetic structure, or (2) a low-spin ferromagnetic structure. As the Néel temperature of the inner layers is lower than the Curie temperature of the surface layer, one would expect a sudden increase of the magnetization at the Néel temperature in the  $M_s$  vs  $T$  curve of the 4 ML annealed film assuming the inner layers have an antiferromagnetic structure. However, this phenomenon has not been observed in Fig. 2. Thus, it is more likely that the inner layers of the 4 ML annealed film have a low-spin ferromagnetic structure.

The decrease of the Curie temperature after annealing can be easily understood according to the suggested model. After annealing, the measured  $T_C$  reflects the Curie temperature of the remaining high-spin ferromagnetic layers. The Curie temperature of the annealed film, therefore, decreases to a value corresponding to 1–2 layers of Fe-Cu alloy, which is determined experimentally to be about 220 K (Fig. 2). On the other hand, the large increase of  $H_c$  after annealing has to be associated with the pit formation. The pits could serve as pinning centers for the domain-wall motion. This also explain why after annealing the  $H_c$  of the 4 ML film is smaller than that of the 3 ML film: there are less pits in the annealed 4 ML film than in the annealed 3 ML film.<sup>16</sup>

Since the magnetic phase transition after annealing is closely connected with the fct→fcc structural relaxation in the inner layers of the Fe films it is worthwhile to discuss the origin of this structural relaxation. In the previous work<sup>16</sup> we have already experimentally proved that the driving mechanism for the pit formation is the surface free energy. How-

ever, the formation of the pits in the Fe/Cu(100) films has not only reduced the total free energy of the system due to the copper diffusion, but also caused a stress relief in the film. The latter can be understood in the following way. Before annealing, the Fe films have a tensile strain in the vertical direction as indicated by the interlayer expansion (Fig. 5). The relief of the stress in the Fe films can be largely accomplished by pit formation, as a considerable amount of strained volume has been removed from the pits in the films. The relaxation of the vertical tensile strain directly results in the change of the structure from fct to fcc in the inner layers of the Fe films, as shown by the  $IV$ -LEED data in Fig. 5. The residual strain manifests itself in the still expanded top layers. Annealing also improves the structural order in the lateral direction. The buckled structure of the Fe films before annealing is replaced by a well ordered fcc-like structure except the Fe-Cu alloyed topmost layers.

However, the formation of the pits might not be the only reason for the fct to fcc structural relaxation. In a recent temperature-dependent  $IV$ /LEED study of the Fe/Cu(100) film, Zharnikov *et al.*<sup>13</sup> have shown that the fct structure of the films tends to relax back to the fcc structure upon heating to a temperature of 370 K, at or below which no pits could be formed. The main difference between the fct to fcc structural relaxation observed in Ref. 13 and in this work, is the reversibility of this structural change. In Ref. 13, the fcc to fct transition is a reversible process as the fct structure will be recovered after the temperature is lowered. In the present work, the fct to fcc transition is a completely irreversible process and the transformed fcc structure is stable at low temperatures. Comparing these two studies, we conclude that the transformation from fct to fcc is a general tendency of the Fe/Cu(100) system upon heating, while the pit formation helps to stabilize the transformed fcc structure.

## V. SUMMARY

In summary, we have achieved a comprehensive understanding of the evolution of the magnetization depth profile of the Fe/Cu(100) films upon thermal annealing. The change of the magnetic properties is closely connected with the annealing-induced structural relaxation. Before annealing, the films are strained and have a buckled fct structure. The fct structure tends to transform to the fcc structure in order to reduce both the strain energy and the magnetic energy. Such a transformation can be accomplished by the pit formation upon annealing. The annealed films have a fcc structure in the bulk layers and a fct structure in the topmost layers. The topmost layers are still expanded, are ferromagnetic and contribute to the measured magnetic signals.

## ACKNOWLEDGMENTS

The authors would like to thank J. Barthel, F. Pabisch, and G. Kroder for their technical support.

- <sup>1</sup>J. Thomassen, F. May, B. Feldmann, M. Wuttig, and H. Ibach, *Phys. Rev. Lett.* **69**, 3831 (1992).
- <sup>2</sup>J. Giergiel, J. Kirschner, J. Landgraf, J. Shen, and J. Woltersdorf, *Surf. Sci.* **310**, 1 (1994).
- <sup>3</sup>S. Müller, P. Bayer, C. Reischl, K. Heinz, B. Feldmann, H. Zillgen, and M. Wuttig, *Phys. Rev. Lett.* **74**, 765 (1995).
- <sup>4</sup>Dongqi Li, M. Freitag, J. Pearson, Z. Q. Qiu, and S. D. Bader, *Phys. Rev. Lett.* **72**, 3112 (1994).
- <sup>5</sup>J. Giergiel, J. Shen, J. Woltersdorf, A. Kirilyuk, and J. Kirschner, *Phys. Rev. B* **52**, 8528 (1995).
- <sup>6</sup>R. D. Ellerbrock, A. Fuest, A. Schatz, W. Keune, and R. A. Brand, *Phys. Rev. Lett.* **74**, 3053 (1995).
- <sup>7</sup>M. Straub, R. Vollmer, and J. Kirschner, *Phys. Rev. Lett.* **77**, 743 (1996).
- <sup>8</sup>B. Gubanka, M. Donath, and F. Passek, *Phys. Rev. B* **54**, R11 153 (1996).
- <sup>9</sup>H. Magnan, D. Chandesris, B. Villette, O. Heckmann, and J. Lecante, *Phys. Rev. Lett.* **67**, 859 (1991).
- <sup>10</sup>M. Wuttig, B. Feldmann, J. Thomassen, F. May, H. Zillgen, A. Brodde, H. Hannemann, and H. Neddermeyer, *Surf. Sci.* **291**, 14 (1993).
- <sup>11</sup>K. Kalki, D. D. Chambliss, K. E. Johnson, R. J. Wilson, and S. Chiang, *Phys. Rev. B* **48**, 18 344 (1993).
- <sup>12</sup>V. L. Moruzzi, P. M. Marcus, and J. Kubler, *Phys. Rev. B* **39**, 6957 (1989); C. S. Wang, B. M. Klein, and H. Krakauer, *Phys. Rev. Lett.* **54**, 1852 (1985).
- <sup>13</sup>M. Zharnikov, A. Dittschar, W. Kuch, C. M. Schneider, and J. Kirschner, *Phys. Rev. Lett.* **76**, 4620 (1996).
- <sup>14</sup>M. Arnot, E. M. McCash, and W. Allison, *Surf. Sci.* **272**, 154 (1992).
- <sup>15</sup>T. Detzel and N. Memmel, *Phys. Rev. B* **49**, 5599 (1994).
- <sup>16</sup>J. Shen, J. Giergiel, A. K. Schmid, and J. Kirschner, *Surf. Sci.* **328**, 32 (1995).
- <sup>17</sup>A. K. Schmid, D. Atlan, H. Itoh, B. Heinrich, T. Ichinokawa, and J. Kirschner, *Phys. Rev. B* **48**, 2855 (1993).
- <sup>18</sup>E. R. Moog and S. D. Bader, *Superlattices Microstruct.* **1**, 543 (1985).
- <sup>19</sup>J. Giergiel, H. Hopster, J. M. Lawrence, J. C. Hemminger, and J. Kirschner, *Rev. Sci. Instrum.* **66**, 3474 (1995).
- <sup>20</sup>Ch. V. Mohan, J. Shen, P. Ohresser, M. Klaua, and J. Kirschner (unpublished).
- <sup>21</sup>J. Kohlhepp, H. J. Elmers, S. Cordes, and U. Gradmann, *Phys. Rev. B* **45**, 12 287 (1992).
- <sup>22</sup>M. Straub, R. Vollmer, and J. Kirschner (unpublished).
- <sup>23</sup>P. A. Serena and N. García, *Phys. Rev. B* **50**, 944 (1994).
- <sup>24</sup>S. S. Manoharan, J. Shen, M. Klaua, H. Jenniches, and J. Kirschner, *J. Appl. Phys.* **81**, 3768 (1997).
- <sup>25</sup>Y. Tsunoda, N. Kunitomi, and R. M. Nicklow, *J. Phys. F* **17**, 2447 (1987).
- <sup>26</sup>M. Wuttig and J. Thomassen, *Surf. Sci.* **282**, 237 (1993);
- <sup>27</sup>S. Müller, P. Bayer, A. Kinne, P. Schmailzl, and K. Heinz, *Surf. Sci.* **322**, 21 (1995).
- <sup>28</sup>A. Kirilyuk, J. Giergiel, J. Shen, M. Straub, and J. Kirschner, *Phys. Rev. B* **54**, 1050 (1996).